Available online at www.sciencedirect.com
SCIENCE DIRECT
Tetrahedron Letters
Tetrahedron Letters 47 (2006) 3637–3640

Nitration reactions of astaxanthin and β-carotene by peroxynitrite

Ryo Yoshioka,[a] Tsutomu Hayakawa,[a] Kumiko Ishizuka,[a] Aditya Kulkarni,[a] Yukimasa Terada,[b] Takashi Maoka[c] and Hideo Etoh[a,*]

[a]*Faculty of Agriculture, Shizuoka University, 836 Ohya, Suruga-ku, Shizuoka 422-8529, Japan*
[b]*Center for Computers and Technology, Meijo University, Shiogamaguchi, Tenpaku, Nagoya 468-8502, Japan*
[c]*Research Institute for Production and Development, Food science, Shimogamo-morimotocho, Sakyo-ku, Kyoto 606-0805, Japan*

Received 6 March 2006; accepted 22 March 2006
Available online 12 April 2006

Abstract—The in vitro reactivities of astaxanthin and β-carotene toward peroxynitrite were investigated and the reaction products after scavenging with peroxynitrite were analyzed. A series of carotenoids substituted with nitro group, 14′-s-*cis*-15′-nitroastaxanthin, 10′-s-*cis*-11′-*cis*-11′-nitroastaxanthin, 14′-s-*cis*-15′-nitro-β-carotene and 10′-s-*cis*-11′-*cis*-11′-nitro-β-carotene, were isolated from the reaction products of carotenoids with peroxynitrite. Carotenoids with nitro derivatives were reported for the first time. These results indicated that astaxanthin and β-carotene could catch peroxynitrite or nitrogen dioxide radical ($^{\cdot}NO_2$) in their molecule to form nitrocarotenoids.

Peroxynitrite, the reaction product of superoxide and nitric oxide, is a powerful oxidant produced by macrophages and neutrophils. Peroxynitrite is known to induce DNA strand scission, protein modification by nitration and hydroxylation and lipid peroxidation in LDL.

In vivo, specifically inside the LDL and in the hydrophobic environment, carotenoids might play an important role in scavenging with peroxynitrite. Carotenoids like zeaxanthin and β-carotene have been studied for their reaction with peroxynitrite,[1,2] however, to our knowledge there is no report of the isolation of nitro compounds in these studies indicating the occurrence of nitration reactions. Our past research have reported some new modes of reactions exhibited by peroxynitrite, which included quenching of peroxynitrite by lycopene in vitro[3] and its consecutive reaction products and mechanisms involved. Astaxanthin, which is found as a common pigment in algae, crustaceans, fish and birds, is reported[4] to be more effective than β-carotene in preventing lipid peroxidation in solution and various biomembrane systems. Furthermore, astaxanthin possesses a different structure than lycopene containing ionone rings and number of oxygen atoms, and might impart some new reaction products. Considering these points, we have concentrated our research on the reactivity of astaxanthin with peroxynitrite and its reaction products. After gaining some useful information, we further extended our work to include β-carotene, which also possesses an ionone ring like that of astaxanthin.

Standard astaxanthin and β-carotene were purchased from Sigma–Aldrich (Japan) Pvt. Ltd, (Shinagawa, Japan). Other reagents were purchased from Wako Pure Chemical Industries (Osaka, Japan). Peroxynitrite was prepared according to the method described in the literature.[5]

All-*trans*-astaxanthin[7] and all-*trans*-β-carotene[8] were reacted with peroxynitrite and the reaction products were analyzed by HPLC.

On HPLC analysis for astaxanthin, three main groups of reaction products were observed, namely fraction A (t_R 0–14 min), B (t_R 14–32 min) and C (t_R 68–76 min). The peaks in fraction A were observed to be of lower λ_{max}, indicating apo-carotenals. The fraction B compounds, which contained the main reaction products, were observed to be the oxygenated products having C-40 skeleton. The compounds in fraction C were 9-*cis*-astaxanthin and 13-*cis*-astaxanthin, respectively, and were identified from the literature values.[6] Further separation of fraction B gave compounds **1** and **2**.

* Corresponding author. Tel.:/fax: +81 54 238 4884; e-mail: acheto@agr.shizuoka.ac.jp

0040-4039/$ - see front matter © 2006 Elsevier Ltd. All rights reserved.
doi:10.1016/j.tetlet.2006.03.139

Compound **1**[9] (t_R 19.4 min, yield 18 mg) showed absorption maxima at 274, 360, 456 nm. The molecular formula was determined to be $C_{40}H_{51}O_6N$ by HR FAB-MS. The partial structure of the end group and the polyene chain in compound **1** were characterized by ^1H NMR and ^{13}C NMR including ^1H-^1H COSY, NOESY, HSQC, and HMBC experiments. The downfield shift of ^{13}C NMR signal at C-15′ (δ 146.1, quaternary carbon) along with the disappearance of methine proton at 15′ position in ^1H NMR, when compared with astaxanthin, clearly indicated that the nitro group was attached at C-15′ position of astaxanthin. Furthermore, the change of the coupling pattern and downfield shift of ^1H NMR signals at H-15 (δ 8.06) and H-14′ (δ 6.36), when compared with astaxanthin, supported the substitution position of the nitro group at C-15′. The steric structure was confirmed by NOESY correlations between CH_3-16/17 and H-7, CH_3-19 and H-7/11, CH_3-20 and H-11/15, CH_3-16′/17′ and H-7′, CH_3-19′ and H-7′/11′, CH_3-20′ and H-11′/14′. Spectral analysis of compound **1**, which was obtained as a major product of the reaction, indicated the structure as 14′-s-*cis*-15′-nitroastaxanthin. Structural optimization of conformational isomers of **1** was performed with ab initio MO methods at the Hartree–Fock (HF/6-31G(d)) level and with density functional theory (B3LP/6-31G(d)) using Gaussian 03 program. The calculated results[10] showed that the established structure **1** is more stable than the straight chain structure, and this was consistent with NOE observation. Therefore, we established the structure as shown in **1** of Figure 1.

Compound **2**[11] (t_R 22.0 min, yield 6.8 mg) showed absorption maxima at 295, 363, 475 nm. The molecular formula was determined to be $C_{40}H_{51}O_6N$ by HR FAB-MS. The partial structure of the end group and the polyene chain in compound **2** were characterized by ^1H NMR and ^{13}C NMR, including 2D experiments. The downfield shift of ^{13}C NMR signal at C-11′ (δ 143.6, quaternary carbon) along with the disappearance of methine proton at 11′ position in ^1H NMR, when compared with astaxanthin, clearly indicated that the nitro group was attached at C-11′. Furthermore, the change of the coupling pattern and downfield shift of ^1H NMR signals at H-10′ (δ 6.41) and H-12′ (δ 7.84) also supported the substitution position of the nitro group at C-11′ position. The steric structure was estimated by NOESY correlations between CH_3-16/17 and H-7, CH_3-19 and H-7, CH_3-16′/17′ and H-7′, CH_3-19′ and H-7′. Spectral analysis of compound **2** indicated the structure as 11′-nitroastaxanthin. The steric structure of 11′-nitroastaxanthin could not be cleared by NOESY analysis. Hence, geometric optimization study[12] was again used in this case to confirm the most stable structure as 10′-s-*cis*-11′-*cis*-11′-nitroastaxanthin, which showed lower potential energy. The final structure has been confirmed as shown in **2** of Figure 1. The detailed steric structure of **2** is shown in Figure 2.

In the analysis of β-carotene, similar to astaxanthin, three main groups of reaction products were observed, namely, fraction A (t_R 0–14 min), B (t_R 14–29 min) and C (t_R 38–42 min). Fraction B on further separation gave two major compounds **3** and **4**.

Compound **3**[13] (t_R 18.2 min, yield 2.9 mg) showed UV–vis absorption maxima at 330, 450 nm. The molecular formula was determined to be $C_{40}H_{55}O_2N$ by HR FAB-MS. ^1H NMR, ^{13}C NMR and 2D experimental analysis showed patterns similar to compound **1**. Moreover, the NOESY results also exhibited identical correlation patterns to that of compound **1** and hence, the final structure of compound **3** was established as 14′-s-*cis*-15′-nitro-β-carotene, as shown in **3** of Figure 1.

Compound **4**[14] (t_R 19.5 min, yield 0.6 mg) on UV–vis spectral analysis showed absorption maxima at 295, 360, 460 nm. The molecular formula was determined as $C_{40}H_{55}O_2N$ by HR FAB-MS. ^1H NMR, including ^1H-^1H COSY and NOESY, values of compound **4** were observed similar to the values of compound **2**. Furthermore, the characterization of methine protons at 10′ and 12′ positions was also done by comparison with the chemical shift values of compound **2**. Therefore, we established the final structure as 10′-s-*cis*-11′-*cis*-11′-nitro-β-carotene, as shown in **4** of Figure 1.

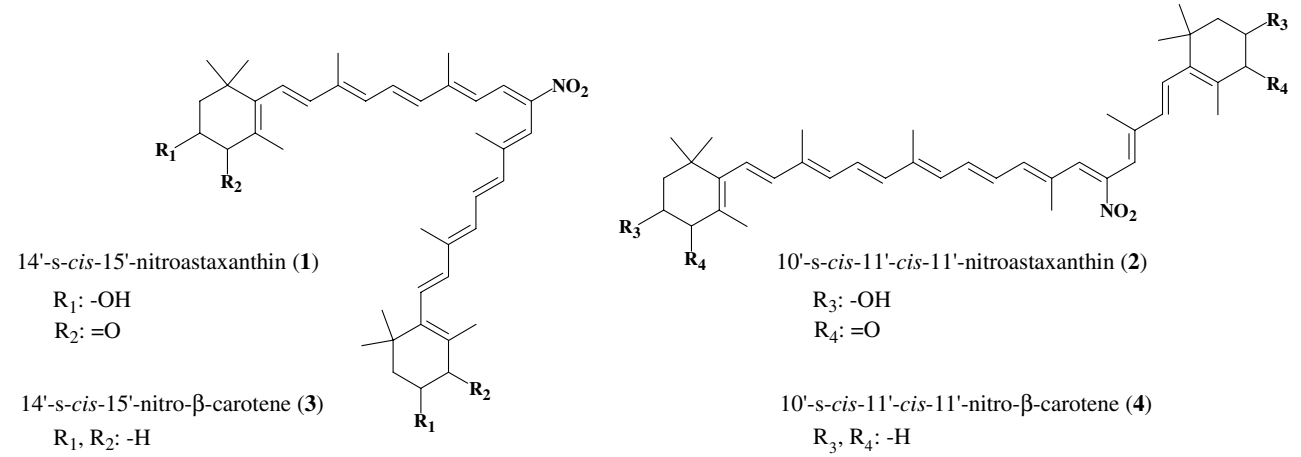

Figure 1. Nitration products of astaxanthin and β-carotene.

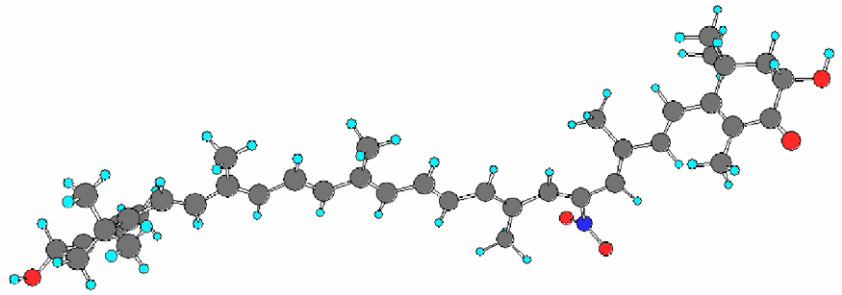

Figure 2. Steric structure of 10′-s-*cis*-11′-*cis*-11′-nitroastaxanthin.

In the present study, nitroastaxanthins and nitro-β-carotenes were isolated from the reaction products of peroxynitrite with astaxanthin and β-carotene, respectively. These results indicated that astaxanthin and β-carotene could catch peroxynitrite or nitrogen dioxide radical ($^{\cdot}NO_2$) in their molecule to form nitrocarotenoids. These informations would be of value for the investigation of the scavenging action of peroxynitrite with carotenoid in vivo. In conclusion, we have for the first time isolated and characterized nitrocarotenoids **1**, **2**, **3**, and **4** from the reaction products of peroxynitrite with astaxanthin and β-carotene.

References and notes

1. Scheidegger, R.; Pande, A. K.; Bounds, P. L.; Koppenol, W. H. *Nitric Oxide: Biology and Chemistry* **1998**, *2*(1), 8–16.
2. Kikugawa, K.; Hiramoto, K.; Tomiyama, S.; Asano, Y. *FEBS Lett.* **1997**, *404*, 175–178.
3. Yokota, T.; Ohtake, T.; Ishikawa, H.; Inakuma, T.; Ishiguro, Y.; Terao, J.; Nagao, A.; Etoh, H. *Chem. Lett.* **2004**, *33*(1), 80–81.
4. Terao, J. *Lipids* **1989**, *24*, 659–661.
5. Niwa, T.; Doi, U.; Kato, Y.; Osawa, T. *J. Agric. Food Chem.* **2001**, *49*, 177–182.
6. Jian-Ping, Y.; Feng, C. *J. Agric. Food Chem.* **1999**, *47*, 3656–3660.
7. All-*trans*-astaxanthin (400 mg) was dissolved in 50 mL of THF (final concentration 5.7 mM). To this, TFA was added in order to makeup the final concentration to 2%, followed by 16 mL of peroxynitrite (final concentration 6.8 mM) and allowed to react for 1 min. Then to the above mixture, 300 mL of $CHCl_3$ and 300 mL of H_2O was added, so as to separate the reaction products into organic and aqueous phases. The whole procedure was performed three times. The organic layer was dehydrated by using anhydrous Na_2SO_4 and concentrated. This organic concentrate was then subjected to HPLC analysis using (Develosil C30-UG-5 ∅4.6 × 250 mm; MeCN:H_2O = 82:18, flow rate: 1mL/min, column temp: 40 °C) column. A more specific separation was done by using (Develosil C30-UG-5 ∅4.6 × 250 mm; MeCN:H_2O = 75:25) column.
8. All-*trans*-β-carotene (200 mg) was dissolved in 50 mL of THF containing 0.3% of TFA, followed by 7.4 mL of peroxynitrite (final concentration 6.4 mM) and reacted for 1 min. The next procedure was performed similar to that in astaxanthin. The organic concentrate was subjected to HPLC analysis using (Develosil C30-UG-5 ∅4.6 × 250 mm; MeCN:MeOH:CH_2Cl_2 = 75:10:15, 1mL/min, column temp: 40 °C) column. A more specific separation was done by using (Develosil ODS-UG-5 ∅4.6 × 250 mm; MeOH) column.
9. 14′-s-*cis*-15′-nitroastaxanthin (**1**) UV–vis λ_{max} (Et_2O) nm 274, 360, 456; high resolution (HR) FAB-MS calcd for $C_{40}H_{51}O_6N + H^+$ 642.3795 found 642.3786; ^1H NMR ($CDCl_3$, 500 MHz) δ 1.20 (H_3-17′, s), 1.21 (H_3-17, s), 1.31 (H_3-16′, s), 1.33 (H_3-16, s), 1.76 (H_3-20′, s), 1.82 (H-2β, t, J = 13), 1.83 (H-2′β, t, J = 13), 1.92 (H_3-18′, s), 1.95 (H_3-18, s), 2.02 (H_3-19, s), 2.04 (H_3-19′, s), 2.16 (H-2α, dd, J = 13, 6), 2.18 (H-2′α, dd, J = 13, 6), 2.18 (H_3-20, s), 4.33 (H-3, dd, J = 13, 6), 4.34 (H-3′, dd, J = 13, 6), 6.00 (H-14, d, J = 13), 6.27 (H-7, d, J = 17), 6.28 (H-10, d, J = 12), 6.30 (H-7′, d, J = 18), 6.30 (H-10′, d, J = 12), 6.36 (H-14′, s), 6.38 (H-8′, d, J = 18), 6.42 (H-8, d, J = 17), 6.47 (H-12, d, J = 15), 6.57 (H-12′, d, J = 15), 6.79 (H-11′, dd, J = 15, 12), 6.94 (H-11, dd, J = 15, 12), 8.06 (H-15, d, J = 13) ^{13}C NMR ($CDCl_3$, 125 MHz) δ 12.7 (C-19), 12.8 (C-19′), 13.6 (C-20), 14.0 (C-18, 18′), 15.2 (C-20′), 26.1 (C-16, 16′), 30.7 (C-17, 17′), 36.8 (C-1, 1′), 45.4 (C-2, 2′), 69.2 (C-3, 3′), 120.0 (C-14′), 124.5 (C-7), 125.4 (C-7′), 126.7 (C-14), 127.1 (C-5), 127.3 (C-5′), 127.4 (C-11′), 129.6 (C-11), 130.1 (C-15), 133.8 (C-10, 10′), 136.5 (C-9), 137.7 (C-12′), 138.1 (C-12), 138.2 (C-9′), 141.5 (C-8′), 141.7 (C-8), 142.7 (C-13′), 146.1 (C-15′), 148.8 (C-13), 161.8 (C-6′), 161.9 (C-6), 200.4 (C-4, 4′).
10. Ab initio calculations were carried out using the Gaussian 03 program (Gaussian Inc., Wallingford, CT, USA, 2004). The starting coordinates of each conformation were generated by the inspection of the molecular model, then they were fully optimized using RHF/6-31G(d) or B3LYP/6-31g(d). The calculations were carried out using a Fujitsu PRIMEPOWER HPC2500 super computer at Information Technology Center, Nagoya University. 14′-s-*cis*-15′-nitroastaxanthin was 21.59 kJ/mol (RHF) or 11.70 kJ/mol (B3LYP) more stable than the straight chain conformation.
11. 10′-s-*cis*-11′-*cis*-11′-nitroastaxanthin (**2**) UV–vis λ_{max} (Et_2O) nm 295, 363, 475; high resolution (HR) FAB-MS calcd for $C_{40}H_{51}O_6N + H^+$ 642.3795 found 642.3777; ^1H NMR ($CDCl_3$, 500 MHz) δ 1.20 (H_3-17′, s), 1.21 (H_3-17, s), 1.32 (H_3-16′, s), 1.33 (H_3-16, s), 1.76 (H_3-19′, s), 1.82 (H-2β, t, J = 13), 1.84 (H-2′β, t, J = 13), 1.89 (H_3-20′, s), 1.94 (H_6-18, 18′, s), 2.02 (H_3-20, s), 2.04 (H_3-19, s), 2.16 (H-2α, dd, J = 13, 6), 2.18 (H-2′α, dd, J = 13, 6), 4.33 (H-3, dd, J = 13, 6), 4.35 (H-3′, dd, J = 13, 6), 6.26 (H-7, d, J = 16), 6.30 (H-10, d, J = 12), 6.33 (H-14, d, J = 12), 6.35 (H-7′, d, J = 16), 6.41 (H-10′, s), 6.42 (H-8, d, J = 16), 6.45 (H-12, d, J = 15), 6.47 (H-8′, d, J = 16), 6.63 (H-15′, dd, J = 13, 12), 6.77 (H-11, dd, J = 15, 12), 6.78 (H-14′, d, J = 12), 6.89 (H-15, dd, J = 13, 12), 7.84 (H-12′, s) ^{13}C NMR ($CDCl_3$, 125 MHz) δ 12.7 (C-19), 13.1 (C-20), 13.9 (C-18′), 14.0 (C-18), 14.3 (C-19′), 14.7 (C-20′), 26.0 (C-16′), 26.1 (C-16), 30.6 (C-17′), 30.7 (C-17), 36.8 (C-1, 1′), 45.3 (C-2, 2′), 69.2 (C-3, 3′), 122.9 (C-10′), 124.1 (C-7), 126.5

(C-11), 126.6 (C-5, 5′), 127.1 (C-7′), 129.1 (C-15′), 131.0 (C-13′), 132.8 (C-14), 134.7 (C-10), 135.9 (C-13, 15), 139.0 (C-8′), 139.4 (C-12), 140.2 (C-12′), 140.5 (C-9), 142.0 (C-8), 143.6 (C-9′, 11′), 144.3 (C-14′), 162.3 (C-6,6′), 200.5 (C-4, 4′).

12. Ab initio calculations (see Ref. 10) showed that 10′-s-*cis*-11′-nitroastaxanthin was 1.78 kJ/mol (RHF) or 12.12 kJ/mol (B3LYP) more stable than 10′,12′-s-*cis* conformation.
13. 14′-s-*cis*-15′-nitro-β-carotene (**3**) UV–vis λ_{max} (Et_2O) nm 330, 450; high resolution (HR) FAB-MS calcd for $C_{40}H_{55}O_2N + H^+$ 582.4311 found 582.4312; ^1H NMR ($CDCl_3$, 500 MHz) δ 1.03 (H_6-16, 17, s), 1.04 (H_6-16′, 17′, s), 1.47 (H_4-2, 2′, m), 1.62 (H_4-3, 3′, m), 1.72 (H_3-18, s), 1.73 (H_3-18′, s), 1.76 (H_3-20′, s), 2.01 (H_3-19′, s), 2.02 (H_4-4, 4′, m), 2.02 (H_3-19, s), 2.17 (H_3-20, s), 5.96 (H-14, d, $J = 12.5$), 6.15 (H-8, d, $J = 16$), 6.16 (H-10, d, $J = 11.5$), 6.16 (H-8′, d, $J = 16$), 6.17 (H-10′, d, $J = 11.5$), 6.24 (H-7, d, $J = 16$), 6.29 (H-14′, s), 6.31 (H-7′, d, $J = 16$), 6.40 (H-12, d, $J = 15$), 6.49 (H-12′, d, $J = 15$), 6.79 (H-11′, dd, $J = 15, 11.5$), 6.96 (H-11, dd, $J = 15, 11.5$), 8.07 (H-15, d, $J = 12.5$) ^{13}C NMR ($CDCl_3$, 125 MHz) δ 12.8 (C-19′), 13.0 (C-19), 13.7 (C-20), 15.3 (C-20′), 19.2 (C-3, 3′), 21.8 (C-18, 18′), 29.0 (C-16, 17, 16′, 17′), 29.7 (C-1, 1′), 33.1 (C-4, 4′), 39.6 (C-2, 2′), 118.8 (C-14′), 125.7 (C-14), 127.8 (C-7), 128.0 (C-11′), 129.1 (C-7′), 129.7 (C-10′), 130.0 (C-10), 130.3 (C-11, 15), 130.5 (C-5, 5′), 135.3 (C-12′), 135.8 (C-12), 137.3 (C-9′), 137.4 (C-8), 137.7 (C-8′), 138.1 (C-6, 6′), 140.2 (C-9), 142.8 (C-13′), 145.6 (C-15′), 149.3 (C-13). The assignments of C-8/8′, C-10/10′ and C-19/19′ may interchange.
14. 10′-s-*cis*-11′-*cis*-11′-nitro-β-carotene (**4**) UV–vis λ_{max} (Et_2O) nm 295, 360, 460; high resolution (HR) FAB-MS calcd for $C_{40}H_{55}O_2N + H^+$ 582.4311 found 582.4293; ^1H NMR ($CDCl_3$, 500 MHz) δ 1.03 (H_{12}-16, 17, 16′, 17′, s), 1.47 (H_4-2, 2′, m), 1.62 (H_4-3, 3′, m), 1.71 (H_6-18, 18′, s), 1.73 (H_3-19′, s), 1.87 (H_3-20′, s), 2.02 (H_4-4, 4′, m), 2.02 (H_3-20, s), 2.03 (H_3-19, s), 6.24 (H_2-8, 8′, d, $J = 16$), 6.25 (H-10, d, $J = 11$), 6.29 (H-10′, s), 6.30 (H-7, d, $J = 16$), 6.31 (H-14, d, $J = 12$), 6.36 (H-7′, d, $J = 16$), 6.43 (H-12, d, $J = 15$), 6.62 (H-15′, dd, $J = 13, 12$), 6.74 (H-14′, d, $J = 12$), 6.75 (H-11, dd, $J = 15, 11$), 6.86 (H-15, dd, $J = 13, 12$), 7.78 (H-12′, s).